

# NUMERICAL ANALYSIS OF THE ENGINE WITH SPARK IGNITION AND COMPRESSION IGNITION

*Grzegorz Budzik, Mariusz Cygnar, Lidia Marciniak-Podsadna, Mirosław Grzelka, Bronisław Sendyka, Antun Stoic*

Preliminary notes

The article presents simulation researches on the combustion process in the four-cylinder testing engine, based on the spark ignition engine Toyota Yaris 1,3 dm<sup>3</sup> which was equipped with two systems of power supply i.e.: fundamental and ignition. Two methods of initiating the combustion process were applied: by spark ignition and, after it was turned off, by means of the ignition dose injection. The researches aimed at revealing the differences in the combustion process and engine performance, above all the changes in pressure that occurred in the cylinder for that kind of two-fuel power supply of the engine. The ignition dose injected into the cylinder was equal to about 5 ÷ 8 % of the general mass of the fuel supplied to the engine. The mass of the fuel injected into the approach collector determined the remaining part, and the direct injection of the fuel took place over several dozen of rotation degrees of the crankshaft before TDC (Top Dead Centre). A spatial grid of the engine's model (pre-processor) was prepared, and also a modification to the source KIVA 3V program was made consisting in taking into account of two systems of injection. It is necessary to mention that the standard KIVA 3V program contains, as a default, only one source of fuel injection.

**Keywords:** two fuel injection systems, spark-ignition and compression-ignition engine

## Numerička analiza motora na paljenje iskrom i paljenje kompresijom

Prethodno priopćenje

U radu se prikazuju istraživanja simulacije izgaranja u testiranom motoru s četiri cilindra, na osnovu motora Toyote Yaris 1,3 dm<sup>3</sup> s paljenjem iskrom i opremljenim s dva sustava napajanja energijom: osnovnim i paljenjem. Primijenjene su dvije metode pokretanja postupka izgaranja: paljenje iskrom i ponovo, poslije isključenja, ubrizgavanje zapaljive doze. Cilj je istraživanja bilo utvrđivanje razlika u postupku izgaranja i radu motora, prije svega promjena tlaka do kojih je došlo u cilindru te vrste motora s dva sustava napajanja energijom. Zapaljiva doza uštrcana u cilindar bila je jednaka otprilike 5 ÷ 8 % ukupne mase goriva u motoru. Gorivo je direktno ubrizgavano tijekom nekoliko desetaka stupnjeva rotacije koljenaste osovine prije dostizanja gornje mrtve točke. Pripremljena je prostorna mreža modela motora (predprocesor), a napravljena je i modifikacija izvornog KIVA 3V programa kako bi se uzela u obzir dva sustava ubrizgavanja. Treba spomenuti da standardni KIVA 3V program ima, po defaultu, samo jedan izvor ubrizgavanja goriva.

**Ključne riječi:** dva sustava ubrizgavanja goriva, motor na paljenje iskrom i paljenje kompresijom

## 1 Introduction

In order to conduct a professional analysis of the gas-dynamic phenomena occurring in the cylinder of the combustion engine, advanced numerical methods enabling virtual modelling of the complex power supply systems construction are applied. To obtain the correctness of the combustion engine working parameters, with the simultaneous fulfilment of the more and more rigorous criteria for cost-effectiveness and environmental performance, it is necessary to prepare and research new constructions of the power supply systems with unconventional solutions, facilitating the work of the combustion engine in two thermodynamic circulations. The numerical analysis conducted by means of the KIVA 3V program consists of the preparation of a model of the process of injection and combustion of homogeneous mixture, which is initiated by means of injection of ignition stream (ignition dose). On the basis of the results of the simulated researches, graphs of the courses of thermodynamic parameters were prepared, such as: pressure, and the temperature in the cylinder, for virtually designed engine working on compression ignition mode. Mathematical models, used in the calculations and descriptions of processes occurring inside the engine cylinder, enable in a satisfactory manner to take into account the real conditions. The correctness of the simulated research results is determined by the quality of the input data, which is obtained by means of real researches. The analysis of the process of the combustion

of fuel-air mixture in the engine with spark initiation and compression ignition requires the application of complex calculated methods, applied in specialist numerical programs [1, 2, 3].

## 2 The range of work simulation

Generally, simulation modeling approach can be used for design, prediction, optimization and process control of engineering systems in a wide range of industrial applications [4, 5].

Considering the wide range of simulation work, it had to be done in detail in order to determine its scope and to define the most important research areas, namely:

- designing a spatial model of the engine supply grid,
- the adaptation of the source code of the KIVA program, designed to take into account two power supply systems and different systems. This alteration is essential, as the standard KIVA 3V program recognizes only one power supply,
- defining, in the calculating procedures, the combustion heat for two fuels, as well as the rate of heat release,
- determination of the basic fuel dose for the indirect fuel injection into the intake ducts, as well as the direct injection of the ignition dose into the cylinder,
- carrying out numerical simulations for the engine working on spark ignition and compression ignition, for a predefined rotational speed of the engine.

### 3 Model geometry of the test engine

Simulation studies were carried out for one of the cylinder test engines working at a speed of 2500 rpm, separately for the spark-ignition and compression ignition modes. The simulation of the injection and combustion in the engine test bench for different ways of burning was made possible by the use of the KIVA 3V program working in 64-bit Linux, which was developed by the National Laboratories in Los Alamos [6, 7, 8, 9]. Fig. 1 shows a general view of the calculation grid of the test engine including the intake and exhaust system, for 90° CA after TDC (Top Death Centre).

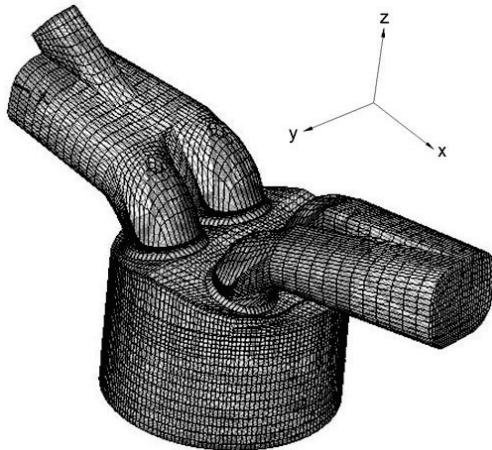


Figure 1 Calculation grid of the engine cylinder for 90° CA after TDC

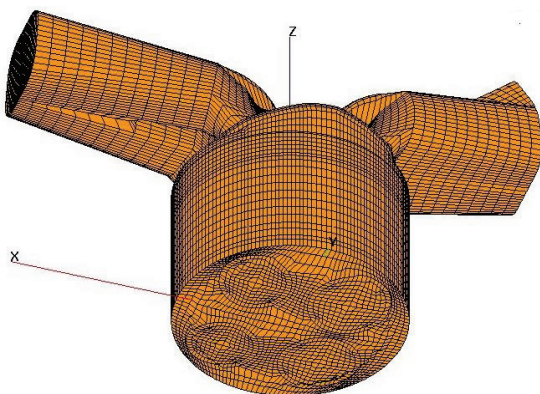


Figure 2 Calculation grid of the engine - view from the cylinder for 90° CA after TDC

The computer simulation required maintaining the real geometrical dimensions of the engine in the calculation grid, namely: the shape of the piston head and combustion chamber and the geometry of the intake and exhaust. The engine cylinder was designed with 47 layers of the *x*-axis layers, 40 horizontal *y*-axis layers and 36 layers of the *z*-axis. The total number of cell calculations for the test engine cylinder is 67 680. Taking into account the geometry of the intake ports and valves, the total number of calculation cells is 104 000. The design of the calculation grid corresponds to the actual geometry of the test engine and is designed in such a way that near the head its density is high, in order to maximize the accuracy of the calculations. Fig. 2 shows a grid view from the cylinder for 90° CA after TDC.

Preparation of the calculation grid of the engine required a lot of modifications during the preparation of

the pre-processor, which took about 70 % of the whole process simulation time. Finally, the engine cylinder was discretized dimensionally as  $X \times Y \times Z = 47 \times 40 \times 36$  calculation cells. Before the actual simulations were conducted some preliminary simulations were used to assess the accuracy of the calculation. Fig. 3 shows a cylinder grid in cross section for 120° CA after TDC.

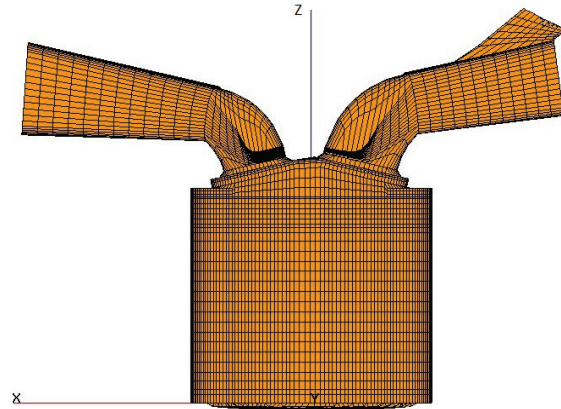


Figure 3 Cross-section calculation grid of the cylinder engine for 120° CA after TDC

The grid was laid down in the Lagrangian [10], due to the possibility of obtaining nearly uniform calculation cell volume. In the case of complex spatial geometry, the calculated cell number is smaller than in the polar coordinate system, which directly affects the shortening of the numerical analysis.

### 4 Parameters of the calculation model

Simulation was executed at the same fuel dose per cycle, where at the two-phase fuel injection it is divided into two stages. The initial conditions applied in simulations are presented below:

- rotational speed 2500 rpm
- general fuel dose for spark ignition 0,022 g
- fuel dose for compression ignition:
  - fuel mass dosed to the intake manifold 0,0208 g
  - mass of the ignition dose of fuel 0,0012 g
- angle of start of fuel injection into the intake manifold 360° CA before TDC
- beginning of ignition for MPI 18° CA before TDC
- duration of ignition 1 ms about 10,8° CA
- angle of start of ignition dose injection 28° CA before TDC
- duration of fuel injection for MPI 80° CA
- duration of injection for CI 3,5° CA
- absolute pressure in the exhaust port 0,1 MPa
- absolute pressure in the intake port 0,13 MPa
- model of turbulence  $\kappa-\epsilon$

The angle of intake valve opening at 4° CA before TDC and closing at 46° CA after BDC was adopted for calculations.

### 5 Modelling of the combustion process in the engine with spark ignition

A computer simulation was carried out of the injection and combustion process for an engine working

in the spark ignition mode, which was based on the PISA module (Piston Engine Simulator) dispensed in the PHOENICS program based on KIVA 3V. The simulation was carried out for the initial conditions determined in Section 4. In the combustion model shown in Fig. 4, the flame front inside the combustion chamber consists of a thin  $\Delta x$  layer separating the unburned mixture from the burned mixture.

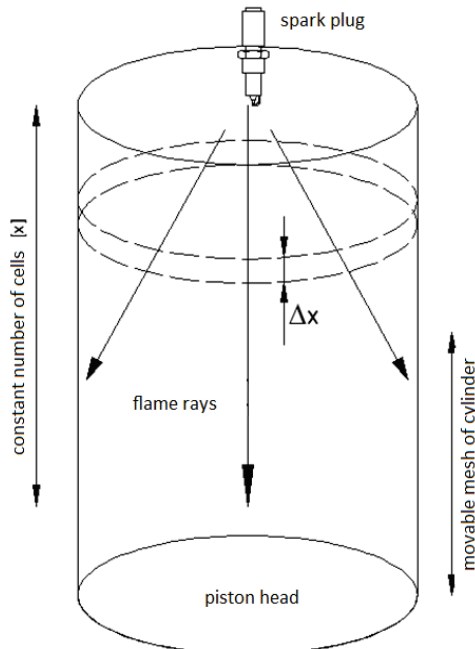


Figure 4 Model of the mixture combustion in an engine with spark ignition

The combustion model used here is a coherent flame model, consisting of a thin flame sheet dividing the fresh gases and the burned gases. This flame propagates from the spark plug towards the piston. Its shape is modelled by turbulence. The average fuel consumption rate is given by:

$$\bar{\dot{\omega}}_F = \beta \cdot \tau \cdot Y \cdot \rho \cdot S \cdot \Omega, \quad (1)$$

where:

- $\beta$  - ratio between the specific heats at constant pressure and at constant volume,
- $\tau$  - rate of fuel in the thermal expansion function,
- $Y$  - average mass fraction of fuel in the fresh charge,
- $\rho$  - average local density of the fresh charge,
- $S$  - laminar flame velocity,
- $\Omega$  - flame area volume density.

The laminar flame velocity is estimated with the Metgalghi and Keck model [3].

### 5.1 Distribution of temperature in the test engine cylinder

Temperature distribution in the engine cylinder is closely connected with the change of temperature of a fuel drop. During the work of the engine with spark ignition in accordance with KIVA 3V, the model assumes that all the fuel droplets leaving the injector are of the

same initial diameter, and the fuel is injected in portions, each of which contains a lot of droplets.

The KIVA 3V software permits presentation of distribution of a number of thermodynamic parameters and mass fractions of chemical components in the cylinder charge, as well as in the intake and exhaust system. Numerical analysis assumed a uniform wall temperature of the combustion chamber and a lower cylinder wall temperature. Figs. 5 ÷ 7 show the charge temperature in the cylinder for the selected angles of the crankshaft rotation.

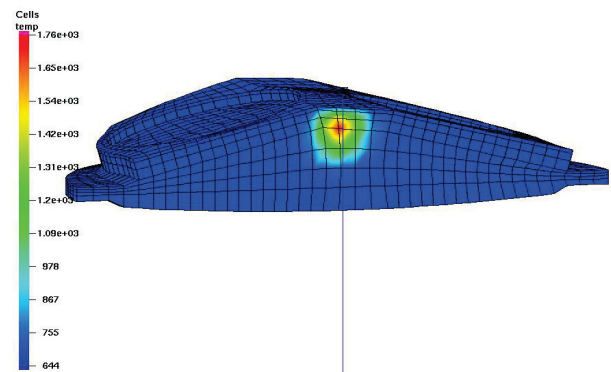


Figure 5 Distribution of temperature in the cylinder at piston position 8° CA before TDC

Fig. 5 shows the initial phase of the flame propagation for 8° CA before TDC and the ignition timing occurring at 15° CA angle before TDC. At the time of initiation of the ignition, the temperature is about 1300 K. The initial mechanism is noted of the formation of the flame which propagates radially in all directions, and other areas are lit from the flame front.

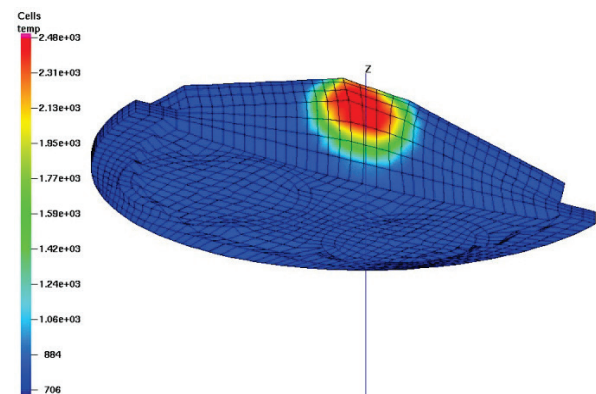


Figure 6 Distribution of temperature in the cylinder at piston position 6° CA before TDC

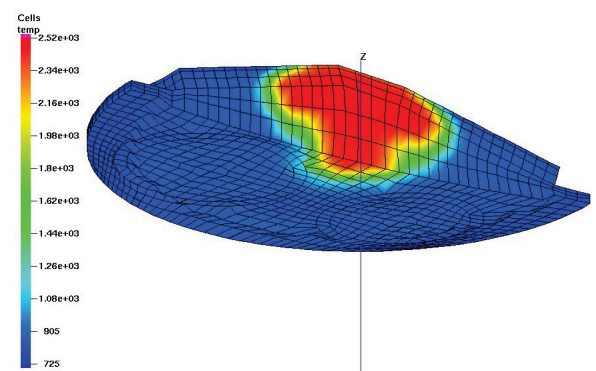


Figure 7 Distribution of temperature in the cylinder at piston position 1° CA before TDC

For this piston position, there is a further development of the radial flame spreading, comprising about 30 % of the combustion chamber volume (Fig. 6).

Fig. 7 presents further development of the flame which propagates in the direction of the piston head and the walls of the combustion chamber in a predetermined model of combustion.

**5.2 Turbulence kinetic energy of the charge in the combustion chamber**

In the calculations by the KIVA model, it was taken into account that the turbulence prevailing in the cylinder depends on the kinetic energy of turbulence. The turbulence in the cylinder is caused by inflow of the fresh charge through the intake channels, as well as the impact of the walls and charge extrusion between the head and the piston during the compression process. Figs. 8 and 9 show the kinetic energy of the turbulence for selected angles of the crankshaft rotation.

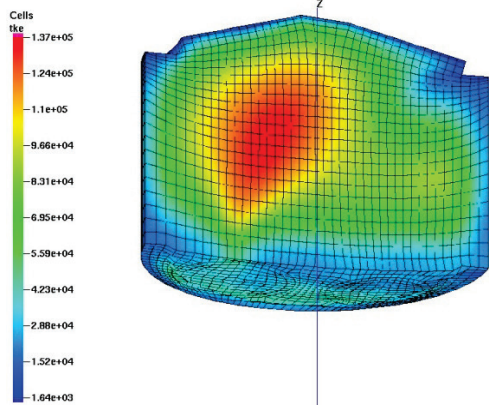


**Figure 8** Kinetic energy of the turbulence at piston position 81° CA before TDC

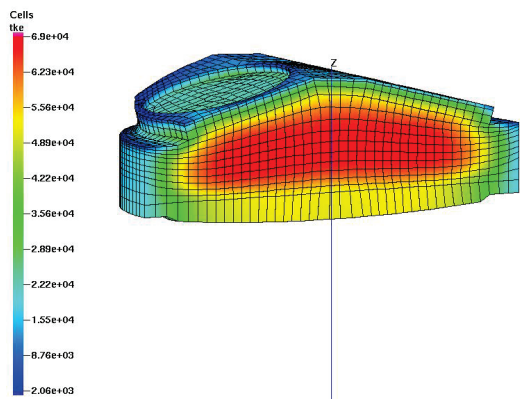


**Figure 9** Kinetic energy of the turbulence at piston position 38° CA before TDC

For the crankshaft position (Fig. 8) where we have the initial phase of the compression process, the kinetic energy reaches the highest values of up to  $1,36 \times 10^5 \text{ cm}^2/\text{s}^2$  and it concentrates in the centre of the engine cylinder.

The kinetic energy of turbulence at 38° crank angle is lower relative to the position 81°. The phenomenon is caused by the reduction of the turbulence speed caused by the interaction of the charge layers (the formation of

larger intermolecular friction forces) and the resistance derived from the combustion chamber walls (Fig. 9).

**6 Modelling of the combustion process in the engine with compression ignition**

Reitz [9] presented a fuel injection model adopted in the KIVA program for spark ignition engines with direct injection. The model takes into consideration fuel atomization, which means a close relation between the drops movement and their disintegration with air movement. It is assumed that a conical fuel jet of  $L$  length and  $h$  thickness is formed at the outflow from the injector (Fig. 10). The mean angle of the injection cone  $2\theta$  is determined by the geometry of the injector needle.

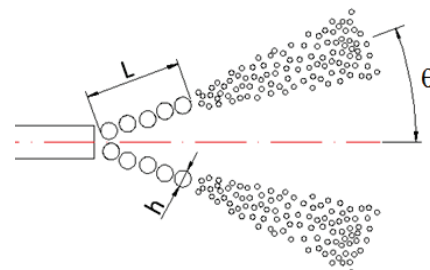


**Figure 10** Scheme of the atomization process of a fuel drop jet

The dimension of the fuel drop portion corresponds with the jet thickness  $h$ . A stochastic injection model is assumed [3]. The speed  $v$  of the fuel jet is determined by the difference between the injection pressure  $p_1$ , the pressure of the surrounds  $p_2$  and fuel density  $\rho_p$ :

$$v = K_v \left[ \frac{2(p_1 - p_2)}{\rho_p} \right]^{0.5}, \tag{2}$$

$$K_v = C \left( \frac{1 - X}{1 + X} \right)^{0.5} \frac{1}{\cos \theta}, \tag{3}$$

$$X = \left( 1 - \frac{2h}{d_0} \right)^2, \tag{4}$$

where:

$d_0$  - diameter of the injector nozzle outlet,

$h$  - thickness of the stream.

**6.1 Distribution of temperature in the test engine cylinder**

The temperature distribution in the cylinder, as in the case of spark ignition, is closely related to the change in the fuel drop temperature. The figures below (Fig. 11 ÷ 13) show the temperature distribution inside the engine cylinder at work in the compression ignition mode.

Fig. 11 shows the distribution of temperature in the cross-section of the working space of the cylinder at piston position 5° CA before TDC. From the temperature distribution it can be seen that the mixture is in the final stage of preparation for the process of self-ignition.

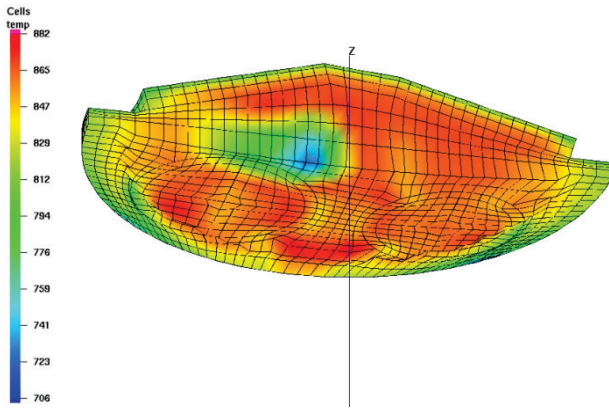


**Figure 11** Distribution of temperature in the cylinder at piston position 5° CA before TDC

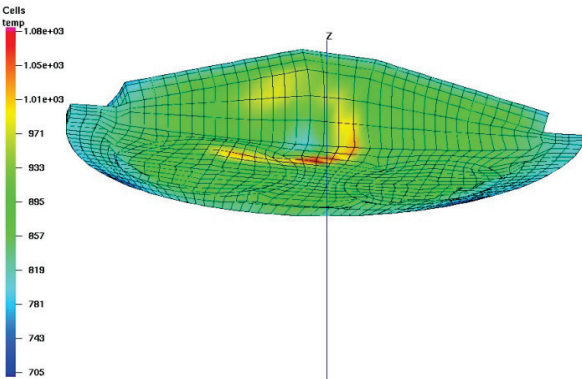


**Figure 12** Distribution of temperature in the cylinder at piston position 1° CA before TDC

Fig. 12 shows the distribution of temperature in the cross-section of the working space of the cylinder at piston position 1° CA before TDC. In this position of the piston at the beginning of the self-ignition process, the mixture temperature of approximately 1000 K was registered.

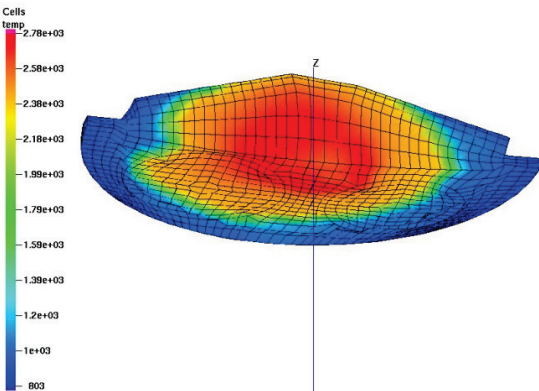


**Figure 13** Distribution of temperature in the cylinder at piston position 4° CA after TDC

Fig. 13 shows the distribution of temperature in the cross-section of the working space of the cylinder at piston position 4° CA after TDC. As a result of flame propagation, a further rapid rise in temperature is noted which, in the central part of the combustion chamber, reaches 2800 K.

## 6.2 Analysis of participation of the gaseous phase

The analysis of the gas phase of ignition dose was carried out on the same model as the simulation of the fuel injection into the intake manifold. Drops breakdown was assumed, as well as the ignition dose streams reflection from the walls and top of the piston, and also a model of charge turbulence was included, which was described earlier for KIVA. The maximum mass of the ignition dose injected into the cylinder is 0,001125 g/cycle, which accounts for 5 % of the total mixture injected to the engine cylinder. Fig. 14 shows the distribution of the gas phase ignition dose for the position of 20° crank angle before TDC. For this position the piston movement of the front ignition fuel spray is observed, towards the centre of the combustion chamber.

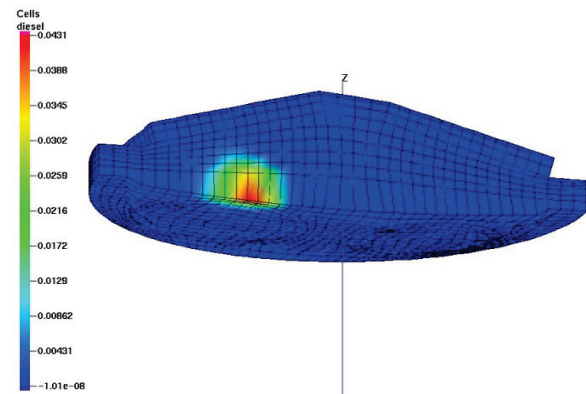


**Figure 14** Participation of the gaseous phase in combustion chamber at 20° before TDC

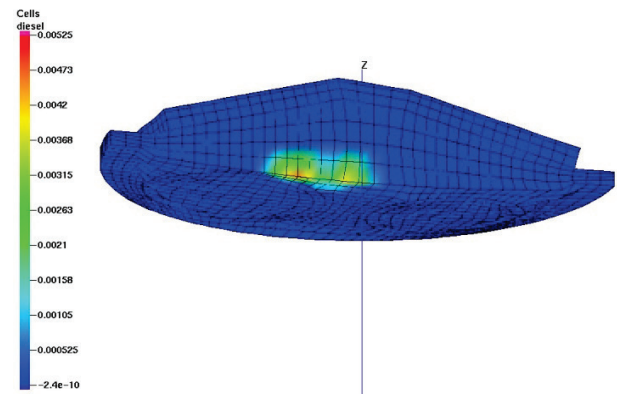


**Figure 15** Participation of the gaseous phase in the combustion chamber at 9° after TDC

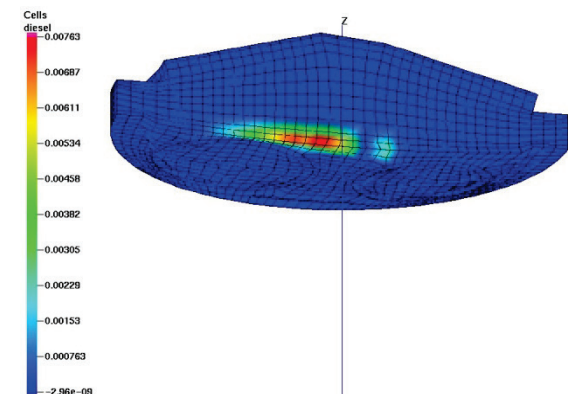


**Figure 16** Participation of the gaseous phase in combustion chamber at 24° after TDC

Fig. 15 shows the distribution of the gas phase ignition dose for the position of  $9^\circ$  crank angle after TDC.

As a result of the ignition dose distribution, which depends primarily on the shape of the injected ignition dose, the shape of the combustion chamber and the injection timing of the ignition dose, for this piston position friction is observed between the front mixture and the piston head (Fig. 15).

Fig. 16 shows fuel film forming for the crank angle  $24^\circ$  after TDC, in contact with the ignition charge of the piston crown.

## 7 Comparison of the pressure and temperature during engine work on spark ignition and compression ignition

For the evaluation of the parameters of an engine working with two ignition systems, performed by means of computer simulation in KIVA 3V program, the comparison of the obtained results was executed. On the graph presented in Fig. 17, the courses of pressure changes in the cylinder of an engine working in both work modes for rotational speed  $n = 2500$  rpm were presented.

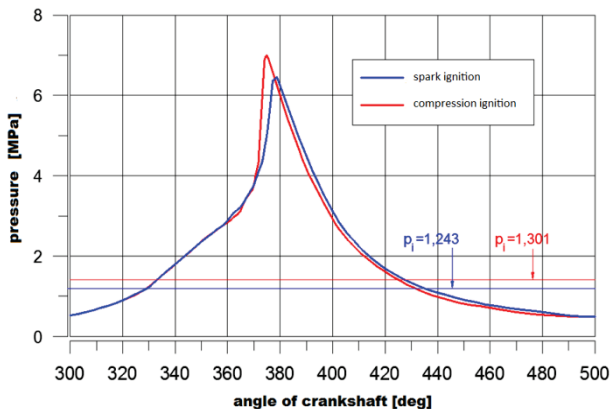


Figure 17 Comparison of the changes of pressure in the cylinder engine working in spark-ignition mode and compression-ignition mode

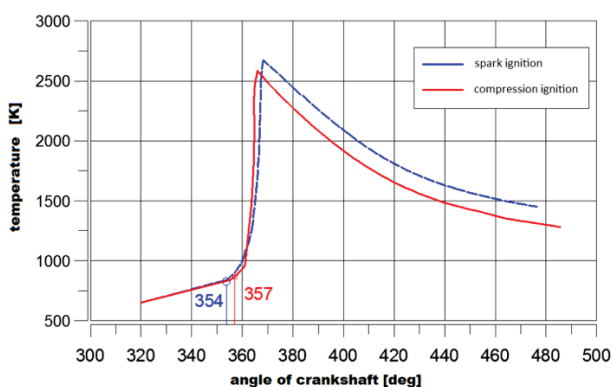


Figure 18 Comparison of the temperature changes in the cylinder of an engine working in spark-ignition mode and compression-ignition mode

On the basis of the pressure course changes the increase was observed by the value of about 0,6 MPa for the working mode with the initiation of the combustion process from the ignition dose in relation to the spark ignition mode.

Subsequently, Fig. 18 illustrates a comparison of the temperature courses inside the test engine cylinder, with the beginning of the combustion process marked.

A higher temperature of up to 2600 K is produced during the combustion charge, as a result of the initiation of the ignition spark combustion. The maximum temperature obtained is lower, and it is obtained for several degrees earlier than the engine working in the spark ignition mode.

## 8 Conclusion

The analysis of the results of the combustion process simulation showed the following results:

1. At an assumed kinetic model of fuel combustion, the combustion process in the initial phase is characterized by very high charge combustion velocity.
2. The maximum combustion temperature reaches the value of almost 3000 K.
3. The auto-ignition of the mixture occurs on the border of the stream of the injected pilot-dose.
4. The combustion process is very short and, for the range  $10 \div 90$  % of the burned fuel, it equals only  $15^\circ$  CA.

## 9 References

- [1] Abraham, J.; Magi, V. GMV - General Mesh Viewer, Los Alamos National Laboratory LA-UR-95-2986, Los Alamos 1995, USA.
- [2] Bracco, F. V. Modeling of Engine Sprays, SAE, Paper 850394, 1985.
- [3] Metghalchi, M.; Keck, J. C. Burning Velocities of Mixture of Air with Methanol, Isooctane and Indolene at High Pressure and Temperature. // Combust. Flame, 1982.
- [4] Ternik P.; Rudolf R. Heat Transfer Enhancement for Natural Convection Flow of Water-Based Nanofluids in a Square Enclosure. // International Journal of Simulation Modelling. 11, 1(2012), pp. 29-39
- [5] Tic, V.; Lovrec, D. Design of Modern Hydraulic Tank Using Fluid Flow Simulation. // International Journal of Simulation Modelling. 11, 2(2012), pp. 77-88
- [6] Adeniji-Fashola, A.; Chen, C. Modelling of Confined Turbulent Fluid - Particle Flows Using Eulerian and Lagrangian Schemes. // International J. Heat Mass Transfer. 33, 4(1990), p. 691.
- [7] Amsden, A. A.; O'Rourke, P. J.; Butler, T. D. KIVA II - A Computer Program for Chemically Reactive Flows with Spray, Los Alamos Labs, LS 11560 MS, 1989.
- [8] Amsden, A. A. KIVA: A KIVA Program with Block-Structures Mesh for Complex Geometries, Los Alamos Labs, LS 12503 MS, 1993.
- [9] Reitz, R. Modeling Atomization Process in High Pressure Vaporization Sprays. // Atomization and Spray Technology. 3, (1987), pp. 309-337.
- [10] Kano, M.; Saito, K.; Basaki, M.; Matsushita, S.; Gohno, T. Analysis of Mixture Formation of Direct-Injection Gasoline Engine. // Gasoline Direct Injection Engine SAE International Congress 2000 USA.

## Authors' addresses

Grzegorz Budzik, Associate Professor, D.Sc., Ph.D. Eng.  
Rzeszow University of Technology  
Powstancow Warszawy Avenue 12, 35-959 Rzeszow, Poland  
tel.: +48 17 8651555, fax: +48 17 8543116  
E-mail: gbudzik@prz.edu.pl

**Mariusz Cygnar, Ph.D. Eng.**

State Higher Vocational School in Nowy Sacz, Technical Institute  
ul. Zamenhofa 1a, 33-300 Nowy Sacz, Poland  
tel.: +48 18 4434545, fax: +48 18 5472609  
E-mail: mcygnar@pwsz-ns.edu.pl

**Miroslaw Grzelka, Assistant Professor, Ph.D. Eng.**

Poznan University of Technology  
Piotrowo 3, 60 - 965 Poznan, Poland  
tel.: +48 61 665 3567, fax: +48 12 6283690,  
E-mail: miroslaw.grzelka@put.poznan.pl

**Lidia Marciniak-Podsadna, MSc. Eng.**

Poznan University of Technology  
Piotrowo 3, 60 - 965 Poznan, Poland  
tel.: +48 61 665 3567, fax: +48 12 6283690  
E-mail: lidia.marciniak@doctorate.put.poznan.pl

**Bronislaw Sendyka, Professor, D.Sc., Ph.D. Eng.**

Cracow University of Technology  
Jana Pawła II 37 Avenue, 31-864 Cracow, Poland  
tel.: +48 12 6283688, fax: +48 12 6283690  
E-mail: bsendyka@pk.edu.pl

**Antun Stoic, Prof. dr. sc., mech. Eng.**

J. J. Strossmayer University of Osijek  
Mechanical Engineering Faculty in Slavonski Brod  
Trg Ivane Brlić Mažuranić 2, 35000 Slavonski Brod  
E-mail: astoic@sfsb.hr